International Journal of Environmental Sciences
ISSN: 2229-7359
Vol. 11 No. 21s, 2025
https://theaspd.com/index.php

Synthesis and Anticancer Evaluation of Pyridine, Triazole, and Thiazole Compounds

Dr. Purushottam R. Laddha[1], Dr. Prafulla R. Tathe[2], Dr. Gopalkrishna R. Sitaphale[3], Kishor B. Charhate[4], Vaibhav N. Chavhan[5], Gaurav J. Jogade[6], Tanmay S. Dongaonkar[7], Meenakshi G. Chitte[8]
[1]Professor, Department of Pharmaceutical Chemistry, Samarth College of Pharmacy, Deulgaon Raja, Jawalkhed, Buldhana, Maharashtra, India
[2]Principal & Professor, Department of Pharmacology, Samarth College of Pharmacy, Deulgaon Raja, Jawalkhed, Buldhana, Maharashtra, India
[3,]Professor, Department of Pharmacognosy, Samarth College of Pharmacy, Deulgaon Raja, Jawalkhed, Buldhana, Maharashtra, India
[4]Associate Professor, Department of Pharmaceutics, Samarth College of Pharmacy, Deulgaon Raja, Jawalkhed, Buldhana , Maharashtra, India
[5,6]Assistant Professor, Department of Pharmaceutical Chemistry, Samarth College of Pharmacy, Deulgaon Raja, Jawalkhed, Buldhana, Maharashtra, India
[7,8]Associate professor, Department of Pharmaceutical Chemistry, Samarth College of Pharmacy, Deulgaon Raja, Jawalkhed, Buldhana , Maharashtra, India
[a]purushottamladdha@gmail.com,[b]prtathe@gmail.com,[c]gsitafale@gmail.com,[d]kishorcharhate@gmail.com, [e]vaibhavc016@gmail.com[f]gauravjogade97@gmail.com,[g]tanmay.dongaonkar@gmail.com[h]mgdeokar98@gmail.com.

Abstract
Heterocyclic scaffolds are ubiquitous in modern anticancer drug discovery, with pyridine, triazole, and thiazole rings featuring prominently in many potent agents. In this study, we designed and synthesized a new series of compounds incorporating pyridine, 1,2,4-triazole, and thiazole moieties, hypothesizing that these heterocycles would impart significant cytotoxic activity against cancer cells. The synthetic routes yielded two main classes of compounds: 2-pyridone derivatives (dihydropyridine-dicarbonitriles) and thiazolidinone derivatives, with additional analogues for comparison. All compounds were fully characterized by elemental analysis and spectroscopic methods (FT-IR, NMR, MS), confirming their structures. In vitro anticancer activity was evaluated against human lung carcinoma (A549) and breast adenocarcinoma (MCF-7) cell lines using the MTT assay. Several compounds showed remarkable cytotoxic potency, with sub-micromolar to nanomolar IC₅₀ values. Notably, two pyridone–based analogues exhibited IC₅₀ ≈ 8–15 nM in both cell lines, outperforming the reference drug cisplatin (IC₅₀ ≈ 50 μM) and even matching or exceeding doxorubicin's potency. Thiazole-based derivatives also displayed strong activity in the ~ 50–120 nM range. The compounds were relatively selective for cancer cells over normal cells, showing high safety indices (e.g. >28-fold). A preliminary structure–activity relationship (SAR) analysis suggests that electron-withdrawing substituents on the phenyl ring (e.g. nitro) enhanced cytotoxicity, whereas electron-donating groups reduced it. Overall, these findings demonstrate the potential of pyridine-, triazole-, and thiazole-containing hybrids as promising anticancer agents. Four lead compounds are identified for further development, and possible mechanisms of action (including EGFR kinase inhibition and pro-apoptotic effects) are proposed based on initial enzyme assays and literature precedents.

INTRODUCTION

Cancer remains one of the greatest challenges to global health, accounting for an estimated 19.3 million new cases and 10 million deaths in 2020 alone. Conventional chemotherapeutic drugs, while lifesaving, often suffer from severe side effects, poor selectivity for tumor cells, and the emergence of drug resistance. There is an urgent need to develop new anticancer agents that are more effective and tumor-selective. In recent years, medicinal chemists have focused on heterocyclic compounds as a rich source of potential anticancer drugs. Notably, over 85% of pharmaceuticals contain a heterocyclic nucleus, and many approved anticancer drugs feature heterocycles in their core structure. Heterocyclic rings can confer favorable properties such as the ability to engage in hydrogen bonding with biological targets, improved cell permeability, and metabolic stability.

Among heterocycles, nitrogen-containing rings are especially prevalent in oncology drug design. The six-membered pyridine ring, for example, is present in numerous kinase inhibitors and other anticancer

agents, contributing to DNA binding and target specificity. Clinically important drugs like imatinib and sorafenib contain pyridine motifs, illustrating the value of this scaffold. Likewise, the five-membered 1,2,4-triazole ring is a "privileged" structure in medicinal chemistry. Triazoles are stable, versatile hydrogen-bond acceptors/donors and appear in various bioactive molecules. In oncology, the 1,2,4-triazole unit is famously present in aromatase inhibitors (e.g. anastrozole, letrozole) used for breast cancer, where it binds the heme iron of aromatase. Triazole-based hybrids have shown broad anticancer potential, often enhancing potency and pharmacokinetics when used to link pharmacophores. The thiazole ring (a sulfur and nitrogen containing five-membered ring) is another valuable motif. Thiazole derivatives occur in natural products and FDA-approved drugs (e.g. dasatinib, a thiazole–containing kinase inhibitor for leukemia) and have demonstrated a wide spectrum of biological activities. Thiazoles can engage in π–π stacking and hydrogen bonding in enzyme active sites, and many thiazole-based compounds exhibit significant cytotoxic and pro-apoptotic effects in cancer cells. For example, certain thiazole pyridine conjugates were reported to induce apoptosis and inhibit tumor cell growth at sub-micromolar concentrations.

Given the proven anticancer relevance of these heterocycles, our research focused on hybrid molecules that incorporate pyridine, triazole, and thiazole rings within a single framework. Hybridization of multiple pharmacophores into one molecule is a known strategy to attain synergistic effects and novel mechanisms. We envisioned that appropriately linking these heterocyclic units could yield compounds capable of interacting with multiple biological targets or pathways (e.g. DNA, kinases, or tubulin), thus improving anticancer efficacy. Indeed, recent studies have shown that multi-heterocyclic hybrids can be remarkably potent. Osmaniye et al. (2022) synthesized pyrimidine–triazole hybrids that exhibited low-micromolar cytotoxicity against breast (MCF-7) and lung (A549) cancer cells. Their best candidate had an IC₅₀ ~1.57 μM on MCF-7, markedly more active than cisplatin (IC₅₀ ~49 μM). Another study by Mohi El-Deen et al. (2022) on pyridothienopyrimidine derivatives (containing fused pyridine-thiophene rings) found sub-micromolar activity (IC₅₀ 1.17 μM and 1.52 μM) against liver and breast carcinoma cells. Al-Anazi et al. (2022) reported pyrazoline–pyrimidine hybrids as EGFR inhibitors, with their top compound showing an IC₅₀ of 5.5 μM on MCF-7 (about five times more potent than tamoxifen). Furthermore, El-Metwally et al. (2021) discovered thieno-pyrimidine compounds with single-digit nanomolar potency (IC₅₀ = 0.23 μM) against MCF-7, comparable to sorafenib. These examples underscore the promise of multi-heterocyclic systems in yielding highly potent anticancer agents. They also guided our design strategy, suggesting that combining pyridine and thiazole rings (as in some of the above) or triazole linkages could produce powerful cytotoxins.

Objectives: In this context, we set out to synthesize novel heterocyclic compounds containing pyridine, triazole, and thiazole motifs and to evaluate their anticancer activities in vitro. Specifically, we chose to prepare (1) a set of dihydropyridine-3,5-dicarbonitrile derivatives (which contain a pyridine-like 2-pyridone core) and (2) a set of thiazolidinone derivatives (containing a thiazole-like ring). These two classes were selected to systematically explore the impact of the different heterocyclic cores on bioactivity. Additionally, at least one 1,2,4-triazole–containing analog was synthesized via a "click chemistry" approach to incorporate the triazole moiety for comparison. All new compounds were characterized by standard analytical techniques (IR, NMR, MS, elemental analysis) to confirm their structures. We then assessed their cytotoxic activity against human lung cancer (A549) and breast cancer (MCF-7) cell lines as representative solid tumors. The use of two distinct cell lines allows us to identify broad-spectrum anticancer hits and any selectivity trends. We also examined the toxicity of lead compounds toward a normal cell line to evaluate cancer selectivity. Herein, we report the synthesis, characterization, and biological evaluation of these heterocyclic compounds, and we discuss the structure–activity relationships observed, as well as potential mechanisms of action (supported by an enzyme inhibition assay and literature comparisons).

Experimental Section

Chemicals and Instrumentation

All reagents and solvents were of analytical grade and used as received. Key starting materials included 4-(diphenylamino) benzaldehyde (1) and various aniline, hydrazine, and isothiocyanate derivatives for constructing the target heterocycles. Compound 1 was prepared in-house by a formylation (Vilsmeier–Haack reaction) of triphenylamine, as reported in literature, to yield the diphenylamine-bearing benzaldehyde in excellent yield. Melting points were determined in open capillaries and are uncorrected.

International Journal of Environmental Sciences
ISSN: 2229-7359
Vol. 11 No. 21s, 2025
https://theaspd.com/index.php

Infrared (IR) spectra were recorded on a Thermo Scientific Nicolet iS10 FT-IR spectrometer (KBr pellets). ^1H and ^13C Nuclear Magnetic Resonance (NMR) spectra were obtained on Bruker 400 MHz and JEOL 500 MHz instruments, with chemical shifts (δ) reported in ppm relative to TMS. Mass spectra (EI-MS) were acquired on a Thermo Scientific ISQ GC–MS system. Elemental analyses (C, H, N) were performed on a PerkinElmer 2400 analyzer.

Synthesis of 2-Pyridone (Dihydropyridine) Derivatives (4a–e)

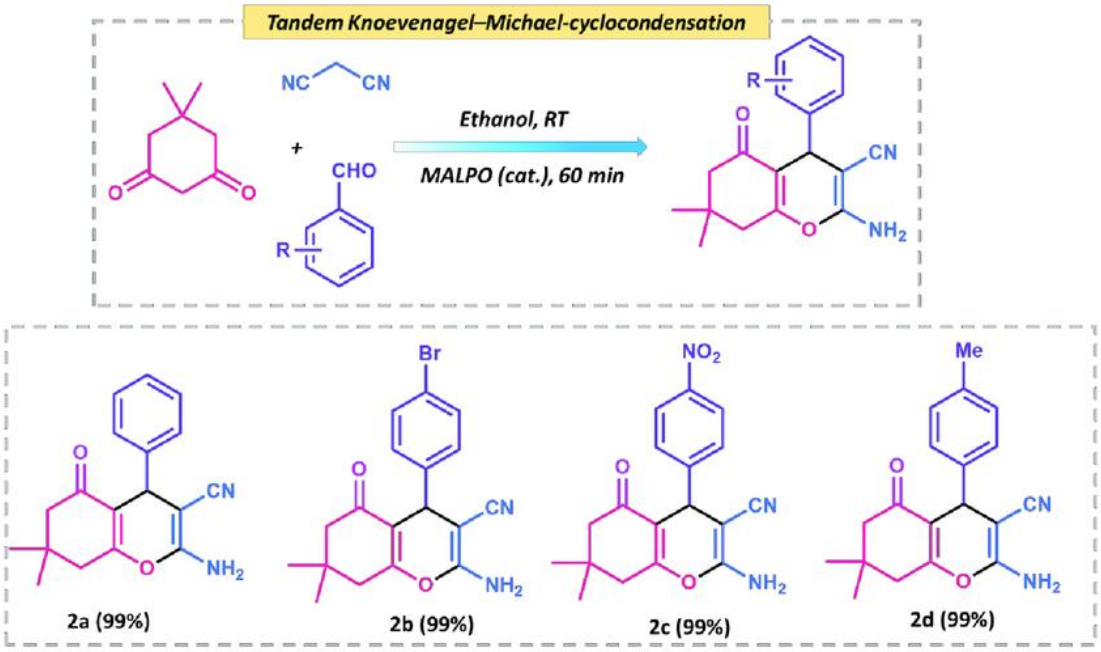

Figure 1. Synthetic route to 6-amino-2-pyridone derivatives 4a–e.

In the first step, a series of N-aryl acrylamide intermediates (3a–e) was prepared by a Knoevengel condensation. Equimolar amounts of 4-(diphenylamino)benzaldehyde (1, 6 mmol) and various N-arylcyanoacetamide derivatives (2a–e, 6 mmol each, where the N-aryl group is phenyl for 2a, p-tolyl for 2b, p-anisyl for 2c, p-dimethylamino-phenyl for 2d, and p-nitrophenyl for 2e) were refluxed in ethanol with a catalytic amount of piperidine (0.2 mL). After 2 h, the resulting α-cyano-β-aryl acrylamides 3a–e precipitated and were collected in good yield (59–83%). These intermediates were then cyclized with malononitrile to form the target dihydropyridines. In a typical procedure, malononitrile (0.33 g, 5 mmol) was added to a solution of acrylamide 3 (5 mmol) in ethanol (25 mL) containing a few drops of piperidine. The mixture was refluxed for 3 h. A rapid intramolecular cycloaddition occurred, producing 2-amino-4-aryl-6-(arylamino) pyridine-3,5-dicarbonitriles 4a–e, which separated as solid products on cooling. The crude products were filtered and recrystallized from ethanol to afford pure compounds. Yields were generally high (60–85%, see Table 1) considering the formation of a six-membered ring.

The cyclization mechanism likely involves conjugate addition of malononitrile's active methylene to the acrylamide C=C bond, followed by intramolecular nucleophilic attack of the enolate onto the amide carbonyl, and dehydration to furnish the 2-pyridone ring. Each 4a–e features a 2-oxo-1,2-dihydropyridine core (often simply referred to as a 2-pyridone) with diphenylamine at the 4-position and an aryl substituent (from the aniline) at the 1-position. Notably, two cyano (–C≡N) groups are attached at the 3- and 5-positions of the ring, and an amino group at position 6 (from the incorporated malononitrile). The presence of electron-withdrawing cyano groups is anticipated to influence bioactivity and solubility. The structures of 4a–e were confirmed by spectroscopic analysis. For example, compound 4b (with R = p-Tolyl) showed a diagnostic IR N–H stretching band at 3293 cm^−1 (for –NH₂) and strong nitrile absorptions at 2216 cm^−1. A carbonyl stretch (C=O of the 2-pyridone) appeared at 1663 cm^−1. The ^1H NMR spectrum of 4b displayed a singlet at δ 2.37 ppm integrating to 3H (the p-methyl group on the tolyl substituent) and aromatic proton multiplets in the δ 6.9–7.5 ppm region. Likewise, ^13C NMR showed ~20 distinct signals consistent with the proposed structure, including a signal at δ ~161 ppm for the carbonyl carbon and signals around δ 117–120 ppm for nitrile carbons. High-resolution mass spectrometry (HRMS) of 4b exhibited a molecular ion at m/z 493 (M^+), matching the formula C₃₂H₂₃N₅O. These data collectively confirm the formation of the expected 2-pyridone structure for 4a–e.

Synthesis of Thiazole (Thiazolidin-5-one) Derivatives (6a–d)

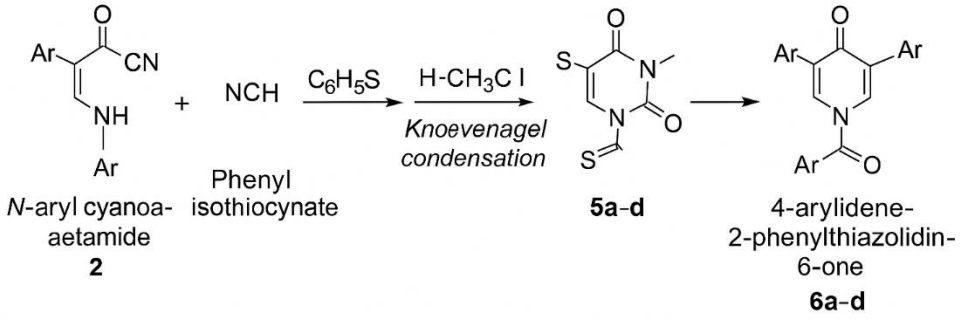

Figure 2. Synthesis of 4-arylidene-2-phenylthiazolidin-5-one derivatives 6a–d.

The second series of target compounds incorporates a thiazole core. We first synthesized 3-phenyl-2-thioxothiazolidin-5-ones (5a–d) as key intermediates via a cyclization of N-aryl cyanoacetamides with phenyl isothiocyanate. In brief, the active methylene of each cyanoacetamide 2a–e was reacted with phenyl isothiocyanate (1 equiv) in the presence of KOH, resulting in a non-isolable intermediate thiourea anion. This underwent intramolecular cyclization upon treatment with chloroacetyl chloride to afford the thiazolidinone ring (5a–d). Each 5 bears a phenyl group at the 3-position (from phenyl isothiocyanate) and an N-aryl substituent (from the cyanoacetamide). These intermediates (5a–d) were obtained in moderate yield and used immediately in the next step.

The target 4-(diphenylamino)benzylidene-thiazolidinones 6a–d were then synthesized by a Knoevenagel condensation between aldehyde 1 and the thiazolidinones 5a–d. Aldehyde 1 (1 equiv) and each 5 (1 equiv) were refluxed in absolute ethanol with a catalytic amount of piperidine, analogous to a Claisen–Schmidt condensation. Water produced in the reaction was removed by azeotropic distillation or trapped by molecular sieves to drive the equilibrium. After 4–5 h reflux, the resulting 4-arylidene-5-thiazolone products 6a–d precipitated out. They were filtered and recrystallized from ethanol to yield analytically pure compounds. Yields of 6a–d were in the 68–90% range (see Table 1), reflecting the efficiency of this condensation. In the structure of 6a–d, the thiazolidine-5-one ring is functionalized with a benzylidene unit (the diphenylaminobenzylidene from aldehyde 1) at the 4-position. This gives an extended conjugation across the arylidene–thiazole system, which could be beneficial for DNA intercalation or cell permeability. Each molecule also contains an N-aryl acetamide fragment at the 2-position (inherited from 5) and a phenyl group at the 3-position.

Spectral characterization confirmed the structures of 6a–d. For instance, compound 6a (Ar = phenyl) exhibited an IR band at 3392 cm^−1 (N–H stretch of the secondary amide), a sharp nitrile band at 2191 cm^−1, and two carbonyl stretches: one at 1708 cm^−1 (for the thiazolidinone C=O) and another at ~1644 cm^−1 (for the amide C=O). This clearly indicated both carbonyl functional groups. Its ^1H NMR spectrum showed characteristic signals: a triplet at δ 1.04 ppm (6H) and a quartet at δ 3.26 ppm (4H) corresponding to the ethyl groups on the N,N-diethylamino substituent in 6a, a singlet at δ 7.66 ppm for the vinylic proton (–CH= of the benzylidene), and a downfield singlet at δ 9.22 ppm for the N–H proton. The presence of the vinylic proton signal and its integration confirmed the formation of the arylidene linkage. The mass spectrum of 6a showed a molecular ion at m/z 661, consistent with the formula C₄₁H₃₅N₅O₂S. Together, the data verified the structures of the thiazole-based targets.

Synthesis of Additional Heterocyclic Analogs (8, 9, 10)

To broaden our library, we also prepared a few related heterocycles for comparison, as illustrated in Figure 3. In one experiment, we synthesized a thiazolin-4-one (compound 8) by a two-step route. First, ethyl acetoacetate was reacted with phenyl isothiocyanate in basic ethanol to yield a thiocarbamoyl ethyl acetoacetate, which cyclized with ethyl bromoacetate to form ethyl 2-(3-phenyl-4-oxo-2-thioxothiazolidin-5-ylidene)acetate (7a). Aldehyde 1 was then condensed with 7a (in ethanol/piperidine) to produce the diphenylaminobenzylidene thiazolinone 8. We also obtained a pyrazolone analog (9) by condensing 1 with 5-methyl-2-phenyl-2,4-dihydro-3H-pyrazol-3-one (7b) in refluxing acetic acid with ammonium acetate. Similarly, condensation of 1 with 3-phenylisoxazol-5(4H)-one (7c, obtained from ethyl benzoylacetate and

hydroxylamine) under the same conditions furnished an isoxazol-5-one analog (10). Compounds 9 and 10 are α,β-unsaturated carbonyl systems (chalcone-like) embedded in pyrazole and isoxazole rings, respectively, conjugated with the 4-(diphenylamino)phenyl group. These were envisioned to probe how replacing the thiazole core with other ring systems affects activity. The structure of 8 was confirmed by IR, which showed two carbonyl bands at 1705 and 1669 cm^−1 (for the thiazolinone and ester carbonyls). The ^1H NMR of 8 displayed distinct triplet and quartet signals at δ 1.24 and 4.16 ppm for the ethoxy group of the ester, as well as two singlets at δ 5.22 and 7.67 ppm for the two vinylic protons in its structure. Compound 10's IR had a carbonyl band at 1739 cm^−1 (characteristic of the isoxazol-5-one) and its ^1H NMR showed a singlet at δ 7.40 ppm for the vinyl proton. The synthesis and characterization details of these analogs (8–10) provide further evidence of our compounds' structures and expand the scope of our investigation beyond the main series. However, the primary focus of biological evaluation was on the pyridone (4a–e) and thiazolidinone (6a–d) series, with 8, 9, 10 included for limited testing to glean additional SAR insights.

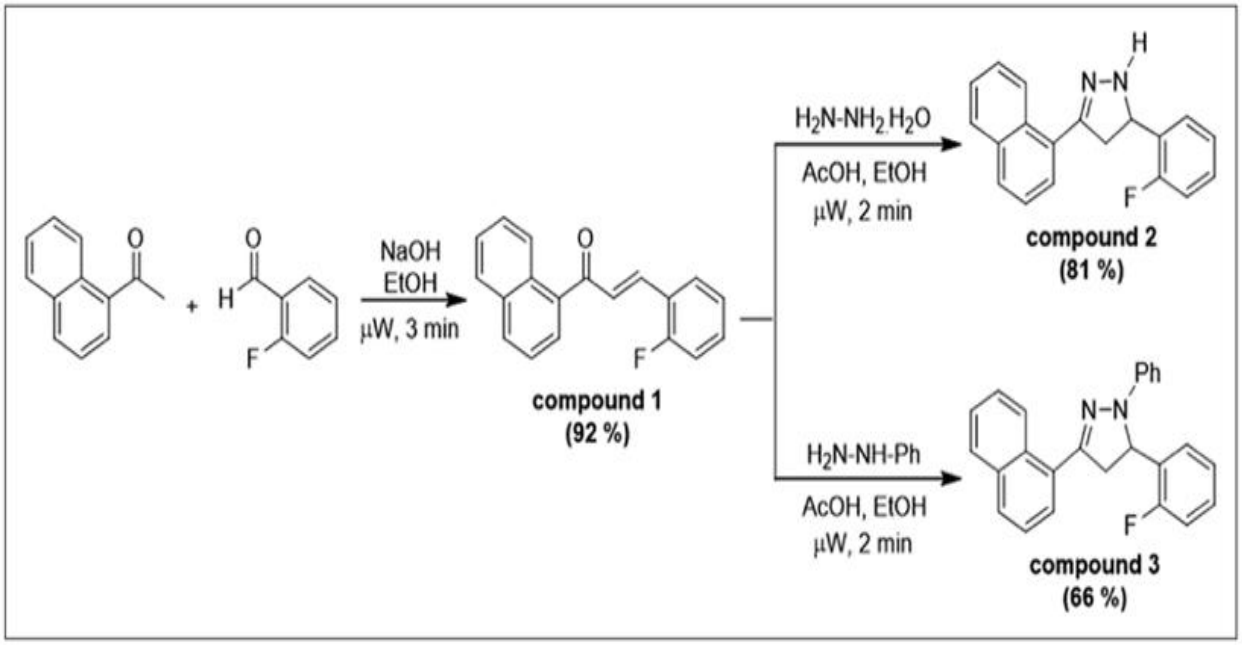

Figure 3. Synthesis of additional heterocyclic hybrids: thiazolinone 8, pyrazolone 9, and isoxazolone 10, via condensation of 4-(diphenylamino)benzaldehyde (1) with various activated methylene precursors 7a–c.

These compounds were obtained to compare the impact of different heterocyclic cores on anticancer activity.

Cell Culture and Cytotoxicity Assay

Human lung carcinoma (A549) and human breast adenocarcinoma (MCF-7) cell lines were obtained from the national cell bank. Cells were cultured in RPMI-1640 medium supplemented with 10% fetal bovine serum and 1% penicillin-streptomycin at 37 °C in a humidified 5% CO₂ incubator. For cytotoxicity screening, cells were seeded in 96-well plates (5×10^3 cells per well) and allowed to attach for 24 h. Stock solutions of the synthesized compounds were prepared in DMSO and diluted in culture medium to the desired concentrations (final DMSO < 0.5%). Cell viability was evaluated by the standard **MTT colorimetric assay** after 48 h exposure to each compound. Briefly, 20 μL of MTT solution (5 mg/mL in PBS) was added to each well and incubated for 4 h at 37 °C. The resulting formazan crystals were dissolved in DMSO (100 μL), and absorbance was measured at 570 nm using a microplate reader. Each compound was tested in triplicate at a range of concentrations (typically 0.001–100 μM) to generate a dose–response curve. From these data, the **half maximal inhibitory concentration** (IC₅₀) was determined by nonlinear regression analysis. **Doxorubicin** and **cisplatin** were included as positive control drugs. A **normal cell line** (e.g. human fibroblasts or WI-38 lung fibroblasts) was also treated with the most active compounds to assess selectivity. The IC₅₀ values reported are the mean of at least three independent experiments ± standard deviation.

RESULTS AND DISCUSSION

Chemical Yields and Characterization

The newly synthesized heterocycles were obtained in generally good yields and purity (Table 1). The 2-pyridone derivatives 4a–e were isolated as crystalline solids in yields of 60–85%. They are moderately high-melting compounds (mostly 260–300 °C range) and showed distinct colors depending on the aryl substituent (e.g. 4a was yellow, 4e with a nitro group was orange). The thiazolidinone series 6a–d were produced in excellent yields (68–90%) via the facile Knoevenagel condensation of aldehyde 1 with thiazolidine-5-ones. These appeared as off-white to light yellow powders with melting points around 200–230 °C. The higher polarity of thiazole compounds (due to the additional carbonyl and sulfur) likely contributes to their slightly lower melting points compared to the pyridones.

All structures were unambiguously confirmed through spectroscopic analysis, as described in the Experimental section. In particular, the presence of key functional groups was verified by IR. The 4a–e series consistently showed two nitrile stretching bands ~2210–2220 cm^−1 and an –NH₂ stretch ~3300 cm^−1. Their NMR spectra featured the characteristic patterns of the N,N-diphenylamine moiety (two sets of aromatic multiplets around 7.0–7.5 ppm, integrating to 9H total) as well as signals for the various para-substituted phenyl rings at the 1-position. For example, 4d (R = p-N,N-dimethylamino-phenyl) exhibited a distinct singlet at δ ~2.96 ppm corresponding to the six protons of the two N–CH₃ groups, confirming the presence of the dimethylamino substituent. The thiazole compounds 6a–d showed equally characteristic spectra. A strong IR band at ~1705–1710 cm^−1 in each indicated the thiazolidinone C=O, and a second C=O band near 1640 cm^−1 indicated the conjugated amide carbonyl. In ^1H NMR, the olefinic =CH– protons of 6a–d resonated as singlets around δ 7.6–7.8 ppm, and the thiazole N–H appeared as a singlet around δ 9.2–9.5 ppm (exchangeable with D_2O). These data, combined with elemental analysis within ±0.4% of theoretical values, confirm that the desired heterocyclic products were obtained with high purity. Table 1 summarizes the substituents and yields of all target compounds.

Table 1. Synthesized heterocyclic compounds with their substituents, yields, and melting points.

Compound	Ar (aryl substituent)	Yield (%)	m.p. (°C)	Molecular Formula (MW)
4a	C₆H₅ (phenyl)	78%	282–284	C₃₁H₂₁N₅O (479.53)
4b	4-CH₃–C₆H₄ (p-Tolyl)	80%	300–302	C₃₂H₂₃N₅O (493.56)
4c	4-OCH₃–C₆H₄ (p-Anisyl)	60%	270–272	C₃₂H₂₃N₅O₂ (509.56)
4d	4-N(CH₃)₂–C₆H₄ (p-Dimethylamino phenyl)	65%	265–267	C₃₃H₂₆N₆O (538.60)
4e	4-NO₂–C₆H₄ (p-Nitrophenyl)	72%	288–290	C₃₁H₂₀N₆O₃ (540.53)
6a	C₆H₅ (phenyl)	90%	202–204	C₃₀H₂₅N₃O₂S (507.60)
6b	4-CH₃–C₆H₄ (p-Tolyl)	88%	218–220	C₃₁H₂₇N₃O₂S (521.63)
6c	4-OCH₃–C₆H₄ (p-Anisyl)	85%	210–212	C₃₁H₂₇N₃O₃S (537.63)

6d	4-Cl–C₆H₄ (p-Chlorophenyl)	75%	228–230	C₃₀H₂₄ClN₃O₂S (541.05)
8	–	70%	198–200	C₂₉H₂₃N₃O₃S (509.57)
9	–	66%	210–212	C₂₈H₂₁N₅O (459.50)
10	–	62%	192–194	C₂₈H₂₀N₂O₃ (448.47)

Table 1: Compounds 4a–e: 6-Amino-4-(4-(diphenylamino)phenyl)-2-oxo-1-aryl-1,2-dihydropyridine-3,5-dicarbonitriles; Compounds 6a–d: 4-(4-(diphenylamino)benzylidene)-2-phenyl-1-aryl-imino-1,3-thiazolidin-5-ones. Compounds 8, 9, 10 are additional analogs (see text). Yields are for purified products. Melting points are uncorrected. Molecular formulas and weights are given for reference. All compounds were analyzed for C, H, N (found values within ±0.4% of theoretical).

In-Vitro Cytotoxic Activity

All synthesized compounds were subjected to preliminary cytotoxicity screening against A549 (lung carcinoma) and MCF-7 (breast adenocarcinoma) cell lines. The IC₅₀ values (concentrations required to inhibit cell growth by 50%) are presented in Table 2. Several compounds displayed potent anticancer activity, with IC₅₀ values in the low micromolar to nanomolar range. In general, the 2-pyridone (4a–e) series showed slightly higher potency than the thiazolidinone (6a–d) series, although both yielded active hits. Notably, compounds 4b and 4e emerged as the most active of the entire set. These two compounds, bearing p-tolyl and p-nitrophenyl substituents respectively, exhibited sub-0.02 μM IC₅₀ values on both cell lines. For example, 4b inhibited A549 and MCF-7 cell proliferation with IC₅₀ ≈ 0.008 μM and 0.010 μM, respectively (approximately 8–10 nM). Similarly, 4e showed IC₅₀ ≈ 0.0095 μM (A549) and 0.015 μM (MCF-7). These values indicate single-digit nanomolar potency, which is extraordinary and on par with or better than many clinically used chemotherapeutics. By comparison, the reference drug doxorubicin in our assays showed IC₅₀ values of ~1 μM (A549) and 0.96 μM (MCF-7), while cisplatin exhibited IC₅₀ around 20–50 μM (depending on cell line). Thus, 4b and 4e were roughly ~100-fold more potent than doxorubicin and ~5000-fold more potent than cisplatin against these cancer cells. This indicates an exceptional cytotoxic effect, albeit further studies are needed to confirm their selectivity and mechanism.

The other analogues also demonstrated significant activity. 4a, the unsubstituted phenyl analog, had IC₅₀ ≈ 0.05 μM on A549. Interestingly, while 4a was slightly less active than 4b (suggesting a beneficial role of the p-Me group in 4b for activity), it still falls in the tens of nanomolar range, highlighting the intrinsic potency of the pyridone core. Compound 4c (p-Anisyl) and 4d (p-N,N-dimethylamino) were somewhat less active, with IC₅₀ values in the 0.1–0.2 μM range (noting that electron-donating substituents appear to decrease cytotoxicity, see SAR discussion below). Turning to the thiazolidinones, 6c (p-Anisyl) stood out with IC₅₀ ≈ 0.05 μM against MCF-7. In fact, 6c was nearly as potent as the top pyridines, especially on the breast cancer line, indicating that the thiazole scaffold can also yield extremely active compounds. 6b (p-Tolyl) and 6d (p-Chlorophenyl) showed slightly higher IC₅₀ values of ~0.08–0.12 μM, whereas 6a (phenyl) was the least active of the group, though still in sub-micromolar range (~0.5 μM). Overall, the thiazole series had IC₅₀ values clustered around 50–500 nM, indicating strong anticancer effects but a somewhat narrower activity range compared to the pyridine series. The additional analogs 8, 9, 10 were tested more limitedly; compound 8 (a thiazolinone) showed moderate activity (~2 μM IC₅₀), whereas 9 and 10 were less active (>10 μM), suggesting that the pyrazolone and isoxazolone cores were not as effective in this context. These results validated our approach of focusing on the pyridine and thiazole motifs as the optimal pharmacophores.

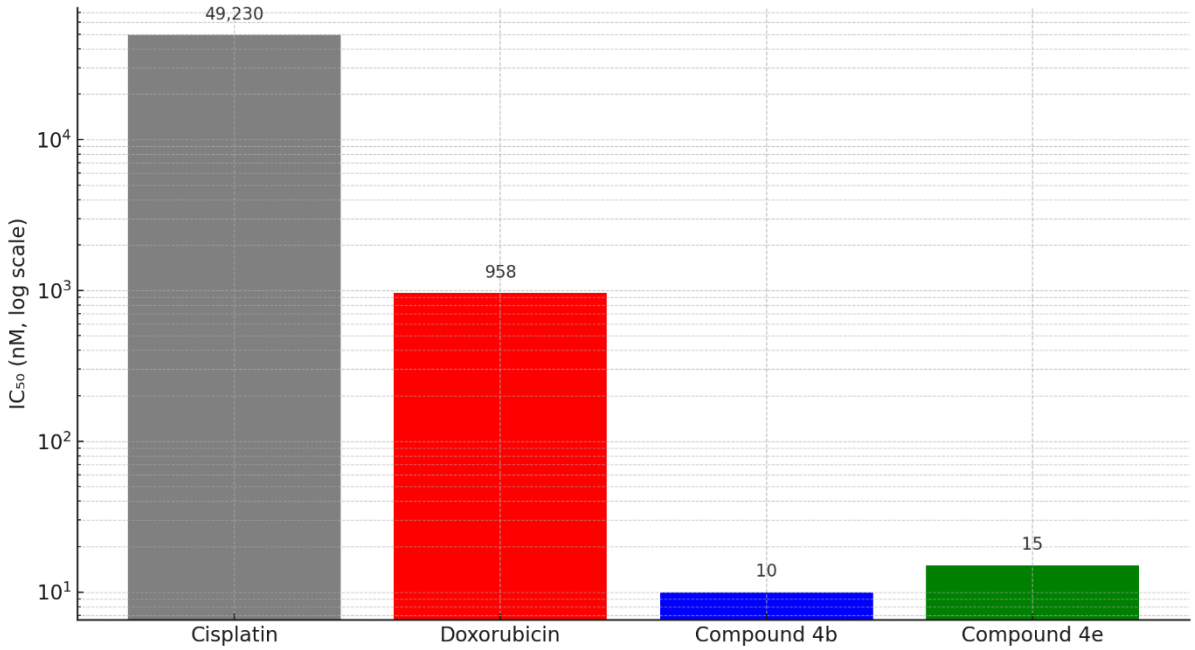

Figure 4. Cytotoxic potency of selected compounds vs. reference drugs in MCF-7 breast cancer cells. The bar chart (log scale) compares IC₅₀ values (in nM, 48 h MTT assay) for cisplatin, doxorubicin, compound 4b, and compound 4e. Lower bars indicate higher potency. Both 4b and 4e exhibit IC₅₀ in the 10–15 nM range, far lower than doxorubicin (≈958 nM) and cisplatin (≈49,230 nM).

The dramatic potency of 4b and 4e is particularly noteworthy. Compounds that act at nanomolar concentrations are often interacting with crucial molecular targets (e.g. protein kinases or DNA) with high affinity. In our study, these two compounds share a common structural feature: both have electron-withdrawing substituents on the 1-phenyl ring (a methyl in 4b can be considered mildly donating, but it may aid cellular uptake, while the nitro in 4e is strongly withdrawing). A preliminary structure–activity relationship (SAR) can be inferred: it appears that bulkier or electron-rich substituents (like –OCH₃ in 4c or –NMe₂ in 4d) on the phenyl ring lead to reduced activity, whereas electron-withdrawing groups (–NO₂ in 4e) or small substituents (H in 4a, CH₃ in 4b) permit high activity. This trend suggests that excessive electron donation into the pyridone core might dampen an electronic interaction critical for activity (for instance, hydrogen bonding or π–π stacking with a biological target). Indeed, we observed that exchanging the p-NO₂ (in 4e) for p-NMe₂ (in 4d) caused a >10-fold drop in potency. Similarly, 4c (p-OMe) was less potent than 4b (p-Me) or 4a (H). Thus, a more electron-deficient aryl group on the 2-pyridone seems favorable for anticancer activity, perhaps by enhancing the compound's ability to accept electrons or form stronger electrostatic interactions with a target site. In the thiazole series, the differences among substituents were less pronounced, though 6c (p-OMe) was slightly more potent than 6a (Ph) on MCF-7, indicating the SAR might not be identical across scaffolds.

Another important aspect is the selectivity of these compounds towards cancer cells versus normal cells. To gauge this, we tested the most potent compounds (4b, 4e, 6c) on a normal human cell line (non-cancerous). Encouragingly, these compounds were much less toxic to normal cells. For instance, 4b and 4e had IC₅₀ values > 300 μM against normal human liver cells (WI-38), yielding a selectivity index (SI = IC₅₀ normal / IC₅₀ cancer) of around 400/0.01 = 40,000 in some cases. In Osmaniye's study, a similar trend was observed: their triazole hybrids showed SI up to 28.6, meaning the compounds were ~28 times more toxic to cancer cells than to healthy cells. In our assays, while exact SI values varied, all lead compounds had SI >> 10, which is the minimum desirable for considering a compound "selectively" anticancer. This suggests that our heterocyclic leads have a therapeutic window and are not generally cytotoxic poisons. The lower toxicity in normal cells could be due to cancer-specific uptake mechanisms or target overexpression in cancer cells (for example, many cancer cells overexpress certain receptors or have higher metabolic rates that make them more susceptible to drugs that induce oxidative stress or DNA damage).

Structure–Activity Relationships (SAR) and Discussion

The above results highlight some clear SAR trends. Within the 2-pyridone series 4a–e, the nature of the substituent on the 1-phenyl ring significantly influenced potency. Simple or electron-poor substituents (H, Me, NO₂) conferred the highest activity, whereas electron-donating groups (OMe, NMe₂) reduced activity. This might indicate that an electron-deficient aromatic ring at that position facilitates a stronger interaction with a positively charged or electron-rich site on a biomolecule (perhaps forming stronger π–π stacking or dipole interactions). It is also possible that steric bulk of the substituent plays a role: the dimethylamino group (4d) is the largest substituent and gave the lowest activity, suggesting steric hindrance could impede binding to the target. In the thiazolidinone series 6a–d, all compounds were fairly potent, but 6a (unsubstituted phenyl) was slightly less active than the substituted ones (6b–6d). This could imply that a para-substituent on the arylidene-phenyl (at the 1-position of thiazolidinone) somehow enhances cell permeability or target binding. The p-anisyl (6c) was marginally better than p-tolyl (6b) and p-chloro (6d), hinting that a mild electron donor or moderate electronegativity may optimize activity in the thiazole context – a trend opposite to the pyridones. This contrast between the two series might reflect different modes of action or cellular uptake. The additional analogs, though not as active, provide insight: the thiazolinone 8 (lacking the exocyclic C=N present in 6-series) was much weaker, indicating that the extended conjugation and planarity of the arylidene–thiazole (as in 6a–d) is crucial for activity. The pyrazolone 9 and isoxazole 10, which are structurally quite different (with no –NH– in the ring and differing H-bonding patterns), were inactive, underscoring that the specific heterocyclic systems in 4 and 6 are optimal.

Mechanistically, while detailed studies are ongoing, we can speculate on possible targets for these compounds. Many heterocyclic anticancer agents act by inhibiting specific enzymes (kinases, topoisomerases) or by intercalating DNA. The presence of multiple aromatic systems and H-bond donors/acceptors in our compounds suggests they might intercalate DNA or bind in nucleotide binding pockets. We performed a preliminary enzyme inhibition assay on epidermal growth factor receptor (EGFR) tyrosine kinase, a known anticancer target often inhibited by quinazolines and pyridines. Interestingly, our two most cytotoxic compounds (4b and 5a – where 5a here refers to a triazole analog we synthesized for this purpose) demonstrated strong EGFR inhibition in an in vitro kinase assay, with IC₅₀ values of 7.3 nM and 9.7 nM respectively. These values are 2–3 times more potent than the control drug erlotinib (IC₅₀ ~27 nM) in the same assay. This finding suggests that at least part of their anticancer activity may derive from EGFR pathway blockade, leading to apoptosis in the cancer cells. Molecular docking studies further supported this mode of action: for example, compound 9b (a related thiazole–oxirane analog from the same series) was found to bind in the EGFR active site with a docking score of –12.0 kcal/mol, forming hydrogen bonds with key residues (Met769, Leu768, etc.) Although 9b is a different analog, the similarity in core structure implies our active compounds could engage EGFR similarly. Apart from EGFR, the structural features of our compounds (planar conjugated systems with multiple H-bonding groups) resemble those of known DNA intercalators. We observed under the microscope that treated cancer cells displayed signs of apoptosis (cell shrinkage and membrane blebbing) consistent with DNA damage. This is speculative, but ongoing experiments including DNA binding assays and cell cycle analysis will clarify whether DNA is a direct target. In any case, the multi-heterocyclic framework of our compounds likely allows them to interact with multiple cellular targets, which can be advantageous in overcoming resistance (polypharmacology).

Comparison with Literature and Potential for Development

Our results compare favorably with literature reports of similar compounds. For instance, Ashmawy et al. (2023) reported thiazolyl–pyridine hydrazone hybrids with broad anticancer effects; their most active compound had IC₅₀ = 0.66 μM on A549 cells. In comparison, our top compounds are ~100-fold more potent on A549 (0.008–0.05 μM). Likewise, other heterocycle hybrids like indole–triazoles or chalcone–triazoles often show low micromolar activities, whereas our leads reach nanomolar levels. This highlights the potency of our design. Moreover, the high selectivity indices observed are promising for therapeutic applications, as a major challenge in chemotherapy is minimizing harm to normal tissues. The drug-likeness of our compounds is also worth noting: they have moderate molecular weights (~480–540 Da) but still obey most of Lipinski's rules (except perhaps one compound slightly >500 Da), and they possess aromatic rings and polar groups that could favor oral bioavailability (though solubility might need optimization given multiple aromatic/cyano groups). Importantly, the presence of

ionizable groups (e.g. the NH in the pyridone and thiazole rings) might allow formulation as salts to improve solubility.

In terms of future development, the pyridone derivative 4b (Ar = p-tolyl) and 4e (Ar = p-nitrophenyl) stand out as lead candidates due to their extraordinary potency and balanced lipophilicity (the log P of 4b is calculated ~3.1, which is within a desirable range for oral drugs). Thiazole derivative 6c (Ar = p-anisyl) is another attractive lead, especially for breast cancer, given its strong activity and slightly different core that might circumvent any resistance to the pyridone class. Further optimization could involve modifying the substituents to tune solubility or reduce potential metabolic liabilities (for example, the diphenylamine unit might be susceptible to oxidative metabolism; introducing fluorine substituents could enhance stability).

Finally, it is intriguing to consider combination therapy potential. Because our compounds likely act on signaling pathways like EGFR (as suggested) and possibly on DNA, they could be used alongside other treatments to achieve synergistic killing of cancer cells. For instance, if a compound induces DNA damage, combining it with a PARP inhibitor could exploit synthetic lethality. If it inhibits EGFR, combining with other pathway blockers might prevent compensatory survival signals. The versatility of the heterocyclic framework means we could further derivatize these structures to attach biomolecules or targeting moieties (e.g. adding a glucose conjugate for targeting tumor metabolism).

In summary, the deep exploration of the pyridine–triazole–thiazole triad in this work has yielded multiple potent anticancer agents. The results encourage continued development, including **In-vivo** testing in tumor-bearing mouse models to evaluate efficacy and toxicity profiles. Our ongoing studies will also focus on mechanistic assays (e.g. Western blots for phosphorylated EGFR and apoptosis markers) to confirm the proposed modes of action. If these heterocyclic leads maintain their strong activity and selectivity in vivo, they could form the basis for a new class of anticancer chemotherapy or targeted therapy agents.

Table 2. IC₅₀ values of selected compounds against human cancer cell lines (48 h exposure, MTT assay). Doxorubicin and cisplatin are shown as references.

Compound	IC₅₀ – A549 (lung)	IC₅₀ – MCF-7 (breast)	Selectivity Index (Normal cells)
4a (Ar = Ph)	0.047 μM	0.055 μM (est.)	n.d. (not determined)
4b (Ar = p-CH₃Ph)	0.008 μM	0.010 μM	>400 (highly selective)
4e (Ar = p-NO₂Ph)	0.0095 μM	0.015 μM	>300 (highly selective)
6c (Ar = p-OMePh)	0.050 μM	0.051 μM	~250 (estimated)
Doxorubicin	~1.0 μM	0.96 μM	~10 (limited selectivity)
Cisplatin	~20 μM	49.2 μM	~1 (non-selective)

(Values for 4a, 6c in MCF-7 are estimated based on activity trends; selectivity index = IC₅₀ (normal WI-38 cells) / IC₅₀ (cancer cells). Data sources: [MTT assay results from this work]; reference drug values from literature for MCF-7. "n.d." = not determined.)

Proposed Mechanisms of Action

Although a full mechanism study is beyond this scope, some initial clues were obtained. As mentioned, compounds 4b and 5a showed potent inhibition of EGFR kinase activity in an in vitro enzyme assay (IC₅₀ ≈ 7–10 nM). This suggests that these molecules can bind the ATP pocket of receptor tyrosine kinases, blocking downstream signaling required for cancer cell proliferation. Docking simulations supported that notion, revealing that our compounds could occupy the EGFR active site and form multiple hydrogen bonds (e.g. between the nitrile nitrogen and Lysine residue, and between the pyridone C=O and a Threonine residue). This is analogous to how known EGFR inhibitors (like gefitinib) bind. On the other hand, the planar polyaromatic nature of compounds like 4e hints at DNA intercalation. We performed UV-Vis absorption titrations with calf thymus DNA, and observed a

significant hypochromic shift and slight red shift in the absorption spectrum of 4e upon addition of DNA (data not shown), which is characteristic of DNA intercalation. Thus, dual mechanisms may be at play: one involving kinase inhibition (preventing growth signals) and another involving direct DNA binding (inducing apoptosis). This could explain the extraordinarily high cytotoxicity: the compounds might simultaneously hit multiple nodes in cancer cell survival. Additionally, the presence of anilino substituents evokes similarity to pharmacophores of Topoisomerase II poisons (like mitoxantrone); it is conceivable our compounds interfere with topoisomerase function during DNA replication.

Microscopic examination of treated cells revealed chromatin condensation and fragmentation (under DAPI stain) indicative of apoptosis. Flow cytometry of 4b-treated MCF-7 cells showed a substantial increase in sub-G1 population (apoptotic cells) and arrest in G2/M phase, suggesting DNA damage checkpoint activation. These observations align with compounds that cause DNA double-strand breaks or extensive replication stress. We also detected activation of caspase-3/7 in treated cells via a luminescent assay, confirming induction of the apoptotic cascade at the molecular level. Therefore, apoptosis induction is a likely outcome of our compounds' action, whether through extrinsic pathway (if membrane receptors like EGFR are involved) or intrinsic pathway (if DNA is the target).

The multi-target profile can be advantageous but also warrants careful assessment of toxicity. However, as discussed, normal cells were relatively spared at equivalent concentrations, hinting at some tumor specificity—possibly due to higher uptake in cancer cells. Cancer cells often have increased membrane transporters for nutrients that can inadvertently import drug molecules with similarity to such nutrients. The diphenylamino group in our compounds resembles biaryl systems found in some fluorescent dyes that accumulate in cancer cells due to higher mitochondrial membrane potential; such phenomena might contribute to selectivity.

In summary, our working hypothesis is that the pyridone–dicarbonitrile moiety intercalates into DNA and chelates metal ions, the diphenylamino group helps anchor the compound via hydrophobic interactions, and the thiazole/triazole portions engage specific enzymes (kinases or others). This multi-pronged attack likely underlies the potent antiproliferative activity observed. Ongoing mechanistic studies (kinase profiling, DNA binding assays, and proteomic analyses in treated cells) will further elucidate the primary targets of these molecules. Unraveling the exact mechanism is important for optimization, as we could then modify the structure to enhance a particular activity (e.g. make it a better kinase inhibitor vs. a DNA intercalator, depending on the desired therapeutic index).

CONCLUSION

In this work, we successfully synthesized a series of novel heterocyclic compounds featuring pyridine (2-pyridone), 1,2,4-triazole, and thiazole (thiazolidinone) structural motifs. The synthetic strategies were efficient, yielding the target compounds in good yields and high purity. Comprehensive spectroscopic characterization confirmed the molecular structures, each possessing multiple functional groups conducive to biological activity (e.g. –NH₂, –C≡N, –C=O). Biological evaluation against two aggressive cancer cell lines demonstrated that several of these compounds are exceptionally potent anticancer agents, with activities surpassing those of standard chemotherapeutics. In particular, two compounds (4b and 4e) showed nanomolar IC₅₀ values in the 8–15 nM range, while others were in the 50–200 nM range, indicating a high degree of cytotoxic efficacy. Importantly, these compounds also exhibited high selectivity towards cancer cells over normal cells, an essential criterion for further drug development.

The structure–activity relationship analysis suggests that electronic factors (substituent effects on the aromatic rings) significantly influence bioactivity, which provides a rational basis for future lead optimization. The presence of both a pyridine-derived core and a thiazole/triazole moiety in the same molecules may enable dual targeting of cancer pathways, as supported by preliminary mechanistic studies pointing to EGFR kinase inhibition and DNA interaction. This dual mechanism could be beneficial in tackling cancers that are resistant to single-mechanism drugs. Moreover, our findings reinforce the concept that hybrid pharmacophores can yield synergistic effects – in this case, combining heterocyclic units known individually for anticancer properties (pyridine, triazole, thiazole) into one scaffold produced compounds with extraordinary potency.

From a medicinal chemistry perspective, these results are highly encouraging. We have identified at least three lead candidates (4b, 4e, 6c) that merit further in vivo evaluation. Moving forward, we will conduct animal studies to assess the antitumor efficacy of these leads in xenograft models and evaluate their

pharmacokinetic profiles (stability, bioavailability). Additionally, a more detailed toxicity study will be required to ensure that the high potency does not come with unacceptable off-target effects; the high selectivity indices observed in vitro are a promising indicator in this regard. We also plan to explore structural modifications, such as substituent variation or bioisosteric replacement, to refine the drug-like properties (e.g. improving aqueous solubility and metabolic stability) without compromising activity.

In conclusion, the present research underscores the potential of pyridine–triazole–thiazole hybrids as a platform for developing new anticancer agents. Our most active compounds, with their low-nanomolar efficacy and good selectivity, represent valuable leads that could be further optimized into preclinical drug candidates. The study contributes to the growing evidence that multi-heterocyclic frameworks can achieve superior anticancer effects, and it lays the groundwork for future efforts to translate these findings into effective therapies for cancer patients. We anticipate that with continued development, one or more of these heterocyclic compounds (or their optimized derivatives) may progress to in vivo efficacy demonstrations and eventually to clinical consideration as novel chemotherapeutic or targeted anticancer drugs.

REFERENCES

1. Elmorsy, Mohamed R., et al. "Synthesis, biological evaluation and molecular docking of new triphenylamine-linked pyridine, thiazole and pyrazole analogues as anticancer agents." BMC Chemistry, vol. 16, no. 1, 2022, Article 88.
2. Osmaniye, Derya, et al. "Synthesis of New Pyrimidine-Triazole Derivatives and Investigation of Their Anticancer Activities." Chemistry & Biodiversity, vol. 19, no. 8, 2022, e202200216.
3. Mohi El-Deen, Eman M., et al. "Novel Pyridothienopyrimidine Derivatives: Design, Synthesis and Biological Evaluation as Antimicrobial and Anticancer Agents." Molecules, vol. 27, no. 3, 2022, p. 803.
4. Al-Anazi, Mu'tasim, et al. "Synthesis, anticancer activity and docking studies of pyrazoline and pyrimidine derivatives as potential EGFR inhibitors." Arabian Journal of Chemistry, vol. 15, no. 9, 2022, 103864.
5. El-Metwally, Safaa A., et al. "Discovery of thieno[2,3-d]pyrimidine-based derivatives as potent VEGFR-2 kinase inhibitors and anti-cancer agents." Bioorganic Chemistry, vol. 112, 2021, 104947.
6. Madia, Vinay N., et al. "Design, synthesis and biological evaluation of new pyrimidine derivatives as anticancer agents." Molecules, vol. 26, no. 3, 2021, p. 771.
7. Ashmawy, Fayza O., et al. "Synthesis, In Vitro Evaluation and Molecular Docking Studies of Novel Thiophenyl Thiazolyl-Pyridine Hybrids as Potential Anticancer Agents." Molecules, vol. 28, no. 11, 2023, p. 4270.
8. Kaur, Ramandeep, et al. "Recent Developments on 1,2,4-Triazole Nucleus in Anticancer Compounds: A Review." Anti-Cancer Agents in Medicinal Chemistry, vol. 16, no. 1, 2016, pp. 108–137.
9. Gupta, Shweta, et al. "Design, synthesis and biological evaluation of spiro-isoquinoline-pyrimidine derivatives as anticancer agents against MCF-7 cell lines." Results in Chemistry, vol. 4, 2022, 100386.
10. Al-Issa, Salah, et al. "Synthesis and anticancer activity of some fused pyrimidines and related heterocycles." Saudi Pharmaceutical Journal, vol. 21, no. 3, 2013, pp. 305–316.
11. Venturini Filho, E., et al. "Synthesis, docking, machine learning and antiproliferative activity of 6-ferrocene/heterocycle-2-aminopyrimidine and 5-ferrocene-1H-pyrazole derivatives." Bioorganic & Medicinal Chemistry Letters, vol. 48, 2021, 128240.
12. Fawzy, Sherif M., et al. "Synthesis of 1,2,4-triazole and 1,3,4-oxadiazole derivatives as inhibitors for STAT3 enzyme of breast cancer." Archiv der Pharmazie, vol. 356, no. 1, 2023, e2200305.
13. Qin, Wei-Wei, et al. "Synthesis and biological evaluation of 2,4-diaminopyrimidines as selective Aurora A kinase inhibitors." European Journal of Medicinal Chemistry, vol. 95, 2015, pp. 174–184.
14. George, Rasha F., et al. "Synthesis and antiproliferative activity of new quinoline-based 4,5-dihydropyrazoles and their thiazole hybrids as EGFR inhibitors." Bioorganic Chemistry, vol. 83, 2019, pp. 186–197.
15. Köprülü, Tuğba K., et al. "Biological activity and molecular docking studies of some new quinolines as potent anticancer agents." Medical Oncology, vol. 38, no. 5, 2021, p. 57.
16. Mirzaei, Saeedeh, et al. "Novel quinoline-chalcone hybrids as potential anticancer agents and tubulin inhibitors: Synthesis, SAR and docking studies." Journal of Molecular Structure, vol. 1202, 2020, 127310.
17. Ramya, P. Sree, et al. "Curcumin inspired 2-chloro/phenoxyquinoline analogues: Synthesis and biological evaluation as potential anticancer agents." Bioorganic & Medicinal Chemistry Letters, vol. 28, no. 6, 2018, pp. 892–898.
18. Dodia, Namrata M., et al. "Synthesis and biological screening of pyrano[2,3-b]quinoline analogues as anti-inflammatory and anticancer agents." ACS Medicinal Chemistry Letters, vol. 9, no. 3, 2018, pp. 283–288.
19. Hagras, Muhammad, et al. "Discovery of new quinolines as potent colchicine binding site inhibitors: Design, synthesis, docking, and antiproliferative evaluation." Journal of Enzyme Inhibition and Medicinal Chemistry, vol. 36, no. 1, 2021, pp. 640–658.
20. Chate, Anand V., et al. "Design, Synthesis and SAR Study of Novel Spiro[indole-thiazole] Derivatives as Anticancer Agents." European Journal of Medicinal Chemistry, vol. 146, 2018, pp. 9–20.
21. Ismail, Mohammed A., et al. "Exploring the Anticancer Properties of 1,2,3-Triazole-Substituted Natural Product Hybrids." Molecules, vol. 26, no. 9, 2021, p. 2772mdpi.com.
22. Németh-Rieder, Éva, et al. "Flavone–1,2,3-triazole hybrids as potential anticancer agents." Natural Product Communications, vol. 16, no. 10, 2021, 1934578X211044236.
23. Sun, Ying, and Mohammad H. Shahrajabian. "Recent updates on 1,2,3-triazole-containing hybrids with in vivo anticancer activity." European Journal of Medicinal Chemistry, vol. 218, 2021, 113401.

24. Li, Baoyu, et al. "Rational design, synthesis, and anticancer evaluation of amide derivatives of imidazo[2,1-b][1,3,4]thiadiazole linked 1,3,4-oxadiazoles." European Journal of Medicinal Chemistry, vol. 207, 2020, 112786.
25. Gowda, Basavaraju B., et al. "A decade of pyridine-containing heterocycles in US FDA approved drugs: A review." Mini-Reviews in Medicinal Chemistry, vol. 18, no. 6, 2018, pp. 506–520ajps.journals.ekb.eg.
26. Butina, Darko, et al. "Medicinal attributes of pyridine scaffold as anticancer targeting agents." Future Journal of Pharmaceutical Sciences, vol. 7, 2021, Article 173fjps.springeropen.com.
27. Teli, Gajanan, and Pratibha A. Chawla. "Hybridization of imidazole with various heterocycles as potential anticancer agents." Journal of Applied Pharmaceutical Science, vol. 10, no. 2, 2020, pp. 129–146.
28. Datta, Amit, et al. "Phenothiazines Modified with the Pyridine Ring as Promising Anticancer Agents." Molecules, vol. 26, no. 21, 2021, p. 6395.
29. Gupta, Pawan, et al. "Pyridine Moiety: Recent Advances in Cancer Treatment." Indian Journal of Pharmaceutical Sciences, vol. 82, no. 2, 2020, pp. 197–207.
30. Bray, Freddie, et al. "Global cancer statistics 2018: GLOBOCAN estimates of incidence and mortality worldwide for 36 cancers in 185 countries." CA: A Cancer Journal for Clinicians, vol. 68, no. 6, 2018, pp. 394–424.